

A Study of Chaotic Behavior of Heat Transfer In Gas-Solid Fluidized Bed

Dr. Jamal Mane'e Al-Rubeai* & Nabeel Majid Aliwi*

Received on:17/5/2009

Accepted on:7/1/2010

Abstract

Fluidized beds are characterized by high heat transfer rates between the bed and internal surfaces and have uniform temperature distribution that can be achieved in fluidized bed systems. In the same time there is a chaotic behavior of hydrodynamic and heat transfer in gas-solid fluidized bed.

Experimental work was carried out in gas-solid (air – sand) fluidized bed to investigate the steady state heat transfer coefficient. The bed column used was (172) mm in diameter and (1000) mm height, fitted with immersed cylindrical heating element of (25.4) mm in diameter. The fluidizing medium was air flowing at different velocities from fixed bed to fluidized bed of (0.006-0.078)m/s, and three different sizes of fine sand particles were used (i.e. 63, 112, and 145 μ m), these average particles diameters were estimated by two methods (Wide and Narrow Range Solids).

A comparison have been done with values of the minimum fluidizing velocity that calculated analytically, empirical, and which got experimentally. The results show a chaotic behavior of hydrodynamic gas-solid fluidized bed.

The heat transfer coefficient and the bed voidage increase with increasing gas fluidizing velocity and the heat transfer coefficient decreases with an increase in particle diameter.

Two empirical correlations are proposed which can calculate wide range solids and narrow range solids based on experimental data. The Nusselt number presented with some dimensionless groups as follows:-

For Wide Range Solids $Nu = 0.81Re^{0.94} Pr^{0.35}$

Where the correlation coefficient (R) was equal to (0.92) and the average absolute relative error was (12.62 %).

For Narrow Range Solids $Nu = 0.45 Re^{0.65} Pr^{0.33}$

Where the correlation coefficient (R) was equal to (0.86) and the average absolute relative error was (24.2 %).

Keywords: - Fluidized Bed, Heat Transfer, Gas-Solid.

دراسة التصرف العشوائي لمعامل انتقال الحرارة في برج الطبقة المميعة غاز-صلب

الخلاصة

تتميز الطبقات المميعة بالغاز (gas-fluidized bed), بإمكانية الحصول على معدلات انتقال حرارة عالية بين الطبقة المميعة وسطوح انتقال الحرارة المغمورة داخليا. لذلك تتصف درجة الحرارة في اعمدة الطبقات المميعة بالانتظام والتي يمكن الحصول عليها في انظمة الاعمدة. في نفس الوقت خواص التصرف العشوائي الهيدروليكية وانتقال الحرارة في الاعمدة

التمميعة غاز - صلب لتحقيق معامل انتقال الحرارة بالحالة المستقرة للطبقة المميعة. عمود التمييع يكون بالابعاد (172 ملم) قطرا و (1000 ملم) ارتفاعا ومجهز بمسخن انبوبي افقي مغمور داخل حشوة من الرمل وبقطر (25.4 ملم) وقد جهز بقدرة كهربائية (4446 واط □ م ٢). في وسط التمييع يكون جريان الهواء بسرور مختلفة تبادء من الطبقة الثابئة الى الطبقة المميعة, وقد اسءءءمء ءقائء الرمل كحشوة وبثلاءة اقءار مختلفة (63,112,145 مايكرومءر), ءم حسب اقءار الحبيباء بطريقتين هما (Wide and Narrow Range Solids). لوءظ ءءصرف العشوائى الهىءرولىكى للطبقة المميعة غاز - صلب من ءلال حسب اقل سرعة ءءمييع (Umf) بمعاءلاء ءءلىلوىة وعملوىة, ومن ءلال ءءارب المءءبرىة. ءءءاء المءءبرىة ءببن ان معامل انتقال الحرارة ءزءاء مع زىاءة سرعة الغازو بءءاقص مع الزىاءة فى قءر الحبيباء. وان الفراغات (Voidage) ءزءاء بىزىاءة سرعة الغاز. معاءلاءان عملىءان ل (Wide and Narrow Range Solids) وءءءنا بالاعءماء على ءءءاء المءءبرىة المسءءصلة واءىضا هءه المعاءلاءان ءربء ال (Nusselt Number) مع بعض المءامىع اللابءىة كما مببب فى المعاءلاءان اءناه:-

$$Nu = 0.81 Re^{0.94} Pr^{0.35} \text{ For Wide Range Solids}$$

هءه العلاءة ءءبرىببىة اعءء معامل ارءبائ (0.92) وءءا مءلق مءوسء مقءاره (% 12.62).

$$\text{For Narrow Range Solids} \quad Nu = 0.45 Re^{0.65} Pr^{0.33}$$

هءه العلاءة ءءبرىببىة اعءء معامل ارءبائ (0.86) وءءا مءلق مءوسء مقءاره (% 24.2).

1. Introduction

Fluidization is a process in which fine solid particles are suspended in a fluid-like state by a carrier medium (typically air) [1].

This method of contacting has some unusual characteristics and fluidization engineering is concerned with efforts to take advantage of this behavior and put it to good use. The first major successful application of gas-fluidized bed techniques, however, was to the engineering of the catalytic cracking process [2,3].

This fluid-like behavior of solid with its rapid, easy and economic transport and its intimate gas contacting is probably the most important property recommending fluidization for industrial operations [4]. One of the most important characteristics of the heat transfer in a fluidized bed is the uniformity of temperature throughout the system, and the high rate of heat transfer

between the internal surfaces and the fluidized bed. An abrupt change in the fluidization speed can be controlled much easier, and because a homogenous distribution exists the temperature implies that all fluidized bed is being processed in the same manner [2, 3].

These are considered as the main reason for choosing the fluidized bed technology to carry out the industrial chemical processes involving the release of large quantities of heat [5].

Hydrodynamic behavior of bubbling fluidized beds is of a chaotic nature. The degree of chaos is quantified by the Kolmogorov entropy, which is a measure of the rate of loss of information in the system (expressed in bits of information per second). Chaotic systems are governed by non-linear interaction between the system variables. Due to this non-linearity, these deterministic

systems are sensitive to small changes in initial conditions and are characterized by a limited predictability. Chaos analysis can be applied to fluidized bed design, scale up, control, and to increase fundamental understanding of the hydrodynamics [6].

Objectives of the Present Research:-

1. Study the chaotic behavior of gas-solid fluidized bed using fine particles.
2. Investigate the heat transfer in gas-solid fluidized bed for different particle diameter; and flow conditions.

2. Experimental Work

2.1 Experiment setup

A schematic diagram of the experimental apparatus is displayed in Figure (1), while Figure (2) shows a photograph for whole experimental set up. The experimental work was carried out in gas-solid (air – sand) fluidized bed to investigate the steady state heat transfer coefficient. The bed column used was (172) mm in diameter and (1000) mm height, fitted with a horizontal heating tube of (25.4) mm in diameter heated electrical with heat flux (4446 W/m²). The fluidizing medium was air flowing at different velocities from fixed bed to fluidized bed of (0.006-0.078)m/s, and three different sizes of fine sand particles were used (i.e. 63, 112, and 145 μm), these particles diameter were estimated by two methods (Wide Range Solids and Narrow Range Solids).

2.2 Bed Material

The experiments were conducted with standard sand that filled the column to a hold up of (30cm) equivalent to (10 kg) charge. Three different charges of particle average sizes were used i.e. (63, 112, and 145 μm).

Particle sizes are calculated as a wide range measuring using the Harmonic mean particle diameter that is determined by sieve analysis which are reported in Table (1) and computed on the basis of the following relationship [2]:-

$$dp = \frac{1}{\sum \left(\frac{x_i}{dp_i} \right)} \dots(1)$$

On the other hand, the particle sizes are calculated as a narrow cut measuring using the geometric mean particle diameter[7]:-

$$dp_m = \sqrt{dp_1 \cdot dp_2} \dots(2)$$

dp_1, dp_2 Where are adjacent sieve openings.

The three particle sizes used are considered within group (A) of Geldart's classification of solid (8).Table (2a, b) shows the physical properties of the bed particles at laboratory temperature for a wide range and a narrow range measuring respectively.

2.3 Experimental Procedure

The general procedure for an experimental run is detailed below:-

1.A charge of the sand sample of (10 kg) weight was introduced to the column up to a packing height of (30 cm) above the distributor plate
 2.The air supply valve was adjusted to allow a level of flow that maintained the bed in the fixed state.
 3.After the minimum fluidization velocity was experimentally determined, the electrical circuit was switched on. The quantity of heat was controlled by variac transformer and measured by an ammeter and voltmeter.
 4.The temperature recording program (by interface system connected computer) was turned on for detecting the temperatures of the eight thermocouples in the system, with a time interval of (10 seconds) between two readings after a constant surface temperature was attained.
 5.The flow valve was readjusted to increase the magnitude of fluidizing velocity to the next level and record the new set of temperature measurements.
 6.For each velocity reading the local heat transfer coefficient was determined using the equation:-

$$h = \frac{q}{A_T (T_s - T_b)} \quad \dots(3)$$

7.The pressure drop and height of the fluidized be were recorded, and the voidage was evaluated from the following

equation:-

$$\varepsilon = 1 - \frac{\Delta P_b}{H (r_s - r_g) g} \quad \dots (4)$$

The results concerned with hydrodynamics and heat transfer in gas-solid fluidized bed and discussion of the experimental work carried out in the research program.

3.1 Chaotic Hydrodynamic Measuring

3.1.1 Minimum Fluidizing Velocity

The transition between the fixed and fluidized bed states is rather gradual and somewhat ill-defined. At a certain velocity, the force of drag on the particles is sufficient to counteract the force of gravity. Beyond this velocity, the resistance to the flow is a maximum and bed pressure drop becomes constant with increasing flow. This velocity is denoted as the minimum fluidization velocity and is a fundamental parameter used to characterize fluidization behavior.

The value of minimum fluidizing velocity is sensitive to particle's shape, density, and size, and it is perhaps the most important parameter used in classifying fluid bed behavior, and yet one of the most difficult to define accurately and to estimate for design purposes without carrying out practical test. There are three basic approaches to obtain equations to calculate the minimum fluidization velocity.

For fine particles, minimum fluidizing velocity is calculated analytically by Carman – Kozeny equation [4]:-

$$u_{mf} = \frac{e_{mf}^3}{5(1-e_{mf})^2} \cdot \frac{\Delta r_b}{r_g m_b H} = \frac{e_{mf}^3}{5(1-e_{mf})} \cdot \frac{(r_s - r_g) g}{m_b S^2} \dots(5)$$

$e_{mf} = 0.4$ & $S = 6/d$ If the particles are spherical with

$$\therefore u_{mf} = 0.00059 \frac{d_p^2 (r_s - r_g) g}{m_g} \dots (6)$$

And minimum fluidizing velocity is calculated empirically by using the relation of Wen and Yu. [9]:-

$$Re_{mf} = (11357 + 0.0408 Ar)^{0.5} - 337 \dots (7)$$

Where the Archimedes number is defined as:-

$$Ar = \frac{d_p^3 r_g (r_s - r_g) g}{m_g^2} \dots (8)$$

And

$$Re = \frac{d_p u_{mf} r_g}{m_g} \dots (9)$$

Therefore:-

$$u_{mf} = \frac{Re_{mf} m_g}{d_p r_g} \dots (10)$$

Another widely used expression obtained empirically by Y. Leva M. [14] for fine particle is:-

$$u_{mf} = 790 \cdot 10^3 d_p^{1.87} (r_s - r_g)^{0.94} m_g^{-0.88} \dots (11)$$

The chaotic behavior in gas-solid fluidized bed can be seen in numerical values of (umf) that are calculated from different equations and practical correlations above [i.e. Equations (6, 7, and 11)]. Table (3.1) and (3.2) contain the experimented and calculated values of minimum fluidizing velocity for different average particle diameters (63,112 and 145µm) and different measuring

techniques (Wide Range Solids and Narrow Range Solids).

It can be noticed that for fine average particle diameters (63,112 and 145µm) the methods used to calculate the values of the minimum fluidization velocity (umf) differ from one size to another (the values of the minimum fluidization velocities become bigger as the particle size increases), and differ from one method to another because of difference in the porosity and density of sand particle. Figure (3) shows the chaotic behavior of minimum fluidizing velocity experimental for different sand particles. In reality, particles in fluidized beds are not distributed uniformly and they even move rather chaotically. The hydrodynamics of gas-solid fluidized beds are a complex phenomenon, determined by the combined effects of formation, motion and interactions of bubbles as well as by the solids behavior [10].

3.1.2 Bed Voidage

The bed voidage (ϵ) is computed from knowledge of pressure drop (ΔP), across bed height (H), by using Equation (4). The average value of voidage fraction is plotted in Figures [(4)-(6)] for different average particle diameters, as a function of fluidizing velocity, the trend of curves shows increase in voidage fraction with increasing velocity.

From this Figures, it can be seen that the gas fluidizing velocity has a large effect on the voidage fraction bed of fine particles. The bed voidage increases with increase in gas fluidizing velocity, and the voidage fraction is more for particle diameter measured as wide range solids in comparison with particle diameter measured in narrow range solids due

to distribution of components which consist of the solids cut of different particle diameters.

3.2 Heat Transfer Coefficient Variation

The heat transfer coefficient is calculated by using Equation (3), on the basis of average temperatures of the whole bed.

It will, therefore, appear that the value of the heat transfer coefficient for an immersed surface will depend on the following effects:-

3.2.1 Gas Fluidizing Velocity

According to Geldart's classification of particles, the Geldart's types "A" particles are the type that has been used in the experiments of this research, which are considered as fine particles. And therefore, for the fine particles, the voidage between the particles is small; the pressure drop in the bed of fine particles is smaller than that of beds containing larger one in spite of the gas velocity in beds of fine particles which is lower than that of beds containing large particles.

It is well known that the gas fluidizing velocity is the characteristic factor which is known to govern the value of the heat transfer coefficient. Figure (7) show the variation in the average surface to bed heat transfer coefficient with the gas fluidizing velocity (u) for different particle average diameters (63,112 and 145 μm) [wide range solids] at heat flux (4446 W/m^2). The figure shows increase in the average surface to bed heat transfer coefficient with increasing the gas fluidizing velocity. As the gas fluidizing velocity increases beyond the minimum fluidizing velocity, the

excess gas will increase the circulation of the particles and increases the frequency of the replacement between the heat transfer surface and the core of the bed which represents the major effect in the increase of the heat transfer coefficient with the gas fluidizing velocity. Figures (8) on for different particle average diameters (63,112 and 145 μm) [narrow range solids] at heat flux (4446 W/m^2).

From these figures, it can be seen that the gas fluidizing velocity has a significant effect on the heat transfer coefficient and that the bubbling character is different from those of beds using small particles. Also the gas flow condition is transformed from transitional to turbulent regime and the interface gas convective component becomes increasingly significant.

3.2.2 Particle Diameter

The heat transfer coefficient will decrease with increasing the particle diameter, as shown in Figure (9); for Wide Range Solids and Narrow Range Solids.

So there is a little change in gas flow rate adjacent to the heat transfer surface, at the same time, the particle convective component of heat transfer is much less relative to the bed of fine particles, and the particle circulation generated is less sensitive to change in the overall gas flow rate than the bed of lower (smaller) mean particle diameter. Thus, both the interface gas convective component and particle convective component of heat transfer are little influenced by the gas flow rate beyond the point of fluidization with large mean particles in bed [12].

3.3 Surface Temperature Variation

The surface temperature is the average of three readings. Figure (10) and Figure (11); show the surface temperature as a function of air superficial velocity from fixed bed to the fluidized bed for different particle sizes. For the sand particle average diameters of (63, 112 and 145µm), it can be seen that the temperature of the heat transfer surface decreases sharply with the increase in the gas velocity from a point in the fixed bed condition to that beyond minimum fluidization velocity.

3.4 Effect of Fluidizing Velocity on Bed Temperature

The bed temperature is the average of two reading Figure (12) and Figure (13), show the bed temperature as a function of air superficial velocity from fixed bed to the fluidized bed for different particle average sizes. It can be seen that the temperature of the heat transfer surface decreases sharply with the increase in the gas velocity from a point in the fixed bed condition to that beyond minimum fluidization velocity.

3.5 Comparison of Experimental Data with Existing Correlations

The various existing correlations reported in the literature have been tested in comparison with the experimental results in the present study. It is necessary to assess the experimental conditions under which data that gave rise to each of these correlations were obtained.

Each correlation reflexes the fluidization conditions especially the solid mixing patterns specific to the equipment in which the experimental data on which it based was derived.

3.5.1 Average Heat Transfer Coefficient

In this section various correlations proposed by other researchers are compared with the experimental data based on the thermal properties of different particle implemented in these earlier investigations.

3.5.1.1 Vreedenberg's Correlation

Vreedenberg [13], made some early extensive studies on heat transfer between a horizontal stainless steel tube and an air fluidized bed at the following conditions: bed temperature [313-613 K], air mass velocity [G= 0.01-0.239 kg/m².s], mean particle diameter [dp= 64-316 µm], particle density [ρs= 1600-5150 kg/m³], and the tube diameter [Dh= 16.9, 33.6 and 51.0 mm]. Experimental results were correlated by:-

$$\frac{hD_h}{k_g} = 0.66 \left[\frac{GD_h r_s (1-e)}{r_g m_g e} \right]^{0.44} \left(\frac{Cp_g m_g}{K_g} \right)^{0.3} \dots(12)$$

$$\frac{Gdpr_s}{mrg} < 2050 \text{ For}$$

The heat transfer coefficient values experimentally obtained in the present study were compared to their corresponding predicted values, and the results are plotted in Figures [(14), (15), (16)] for wide range solids and Figures [(17), (18), (19)] for narrow range solids, where the (45°) line represents zero deviation from the experimental results. It can be seen that the correlation under-predicts the data with a deviation% for different particle sizes of (63, 112 and 145µm) for wide range solids are (50, 31 and 32), and narrow range solids are (28, 44 and 40).

3.5.1.2 Andeen and Glicksman Correlation

The correlations of Andeen et al. [14], in conjunction with the experimental data are examined in Figures [(14), (15), and (16)] for wide range solids and Figures [(17), (18), (19)] for narrow range solids. It is noticed that the deviation between the present experimental data and the predicted values for different particle sizes of (63, 112 and 145µm) for wide range solids are (45, 33 and 27), and narrow range solids are (26, 20, and 30).

$$\frac{hD_h}{K_s} = 900(1 - e) \left[\left(\frac{GD_h r_s}{r_s m_s} \right) \left(\frac{m^2}{d_p^3 r_s^2 g} \right) \right]^{0.326} Pr^{0.3} \dots (13)$$

Figures [(14), (15), (16)] for wide range solids and Figures [(17), (18), (19)] for narrow range solids. Shows the comparison of the experimental and predicted values of two correlations.

3.6 Correlation of Data

In the absence of reliable methods for determining the individual components of heat transfer, empirical formula are used to calculate heat transfer coefficient (practically coinciding with the packet mode when sufficiently different particles are fluidized at moderate temperatures).

In this study on heat transfer between a horizontal immersed tube and a bed fluidized by air at moderate temperatures, it is well proven that the Reynolds number and Prandtl number are a good characteristic dimensionless group for (h); to summarize our experimental; the data following correlation is proposed:-

$$Nu. = C_1 A^{C_2} B^{C_3} \dots (14)$$

The constant C₁ and the powers in the

above equation were calculated using the method of Quasi – Newton on computer program.

4. Conclusions

The following conclusions can be drawn from the present experimental work as:-

- 1.The value of tube-bed heat transfer coefficient increases with an increase in the value of superficial gas velocity and attains a maximum at some intermediate value.
- 2.With a given bed of the solid particle, the heat transfer coefficient increases as the average particle diameter decreases.
- 3.The chaotic behavior of minimum fluidizing velocity for different fine sand particles (63,112 and 145 µm) is shown clearly when three different methods are used to estimate the minimum fluidizing velocity.
- 4.The bed voidage was found to increase with increase in fluidizing velocity.
- 5.The values of heat transfer coefficient estimated based on particle diameters measured as wide range solids are larger than the values estimated based on particle diameters measured as a narrow range solids.
- 6.The values of the Nusslet number were shown to increase slightly with the increase in Reynolds number.
- 7.A comparison of experimental heat transfer coefficients with several existing correlations proposed by various authors, showed a large variation between them, when tested against typical condition used in our experiments.
- 8.A correlation for heat transfer coefficients is proposed on the

basis of the experimental data for fine particle sand.

For Wide Range Solids

$$Nu = 0.81 Re^{0.94} Pr^{0.35}$$

For Narrow Range Solids

$$Nu = 0.45 Re^{0.65} Pr^{0.33}$$

5. References

- [1]. Peter Blomgren, Antonio Palacios, and Bing Zhu, "Bifurcation Analysis of Bubble Dynamics in Fluidization Beds" (2007).
- [2]. Kunii, D., and Levenspiel, O., "Fluidization Engineering", John Wiley Company, New York, (2005).
- [3]. Botterill, J.S.M., and Denloye, A. O.O., "Gas Convective Heat Transfer to Packed and Fluidized Beds", AIChE J. Symposium Series, Vol. 176, No. 74, PP. (144–202), (1978).
- [4]. Davidson, J.F., Clift, R., and Harrison, D., "Fluidization", Academic Press, London, (1985), P. (1-10,474).
- [5]. Benjamin, T.F, Fun, L.T., and Hwang, C.L., "A Model of Heat Transfer in Fluidized Beds", Trans. of the ASME, J. Heat Transfer, PP. (105-110), (1972).
- [6]. Schouten, J.C., Vander Stappen, M.L.M., and Van Den Bleek, C.M. "Scale-Up of Chaotic Fluidized Bed" Chem. Eng. Vol. 51, No. 10, pp. 1991-2000, (1996).
- [7]. Peerler, J.P.K., and White Head, A.B., "Solids Motion at Horizontal Tube Surfaces in a Large Gas-Solid Fluidized Beds", Chem. Eng. Sci., Vol. 37, No., PP. (77–82), (1982).
- [8]. Geldart, D., "Types of Gas Fluidization", Powder Technology, Vol. 7, PP. (282 - 292), (1973).
- [9]. Wen, G.Y., and Yu, Y.H., AIChE Journal, V.12, P.610, (1966).
- [10]. Van der Stappen M. L. M. (1996), "Chaotic Hydrodynamics of Fluidized Beds", PhD thesis, Delft University of Technology, The Netherlands.
- [11]. Leva M., "Fluidization", McGraw-Hill, New York, 1959.
- [12]. Botterill, J.S.M., "Fluid Bed Heat Transfer", Academic Press, London and New York, (1975), P. (2, 147, 22&242).
- [13]. Vreedenberg, H. A., Chem. Eng. Sci, V.9, p.52-60, (1958) [Incited in saxena et al., 1978].
- [14]. Andeen, B.R. and Glicksman, L.R., "Heat Transfer to Horizontal Tubes in Shallow Fluidized Beds", ASME-A.I.Ch.Eng. Heat Transfer Conference, Paper No. 76-HT-67, St. Louis, MO, August 9-11 (1976).

Table (1) Size Distribution of Sand

Adjacent sieve openings (μm)	Average diameter d _{pi} (μm)	Mass fraction of solids retained x _i		
212 – 150	181	---	---	0.34
150 – 140	145	---	0.25	0.36
140 – 125	132.28	0.13	0.20	0.1
125 – 100	112.5	0.17	0.30	0.1
100 – 75	87.5	0.20	0.15	0.1
75 – 53	64	0.27	0.1	---
53 – 25	39	0.22	---	---
$d_p = \frac{1}{\sum \frac{x_i}{d_{pi}}} \mu m$		63	112	145

Table (2a) Properties of Bed Particles, Wide Range Solids

d _p (mm)	(kg/m ³) ρ _s	k(W/m,K)	C _p (J/kg.K)
63	2358	1.87	860
112	2331	1.87	860
145	2300	1.87	860

Table (2b) Properties of Bed Particles, Narrow Range Solids

d _p (mm)	(kg/m ³) ρ _s	k(W/m,K)	C _p (J/kg.K)
63	2318	1.87	860
112	2300	1.87	860
145	2272	1.87	860

Table (3) The Values of Experimental and Calculated Minimum Fluidization Velocity, Wide Range Solids

Particle Diameter μm	Minimum Fluidizing Velocity						
	Calculated Equ.(6) (m/s.)	Calculated Equ.(7) (m/s.)	Calculated Equ.(11) (m/s.)	Experimental (m/s.)	% Error Equ.(6)	% Error Equ.(7)	% Error Equ.(11)
63	0.016	0.017	0.019	0.021	23.8	19.05	9.5
112	0.025	0.026	0.028	0.030	16.66	13.33.	6.66
145	0.031	0.033	0.032	0.036	13.88	8.33	11.11

Table (4) The Values of Experimental and Calculated Minimum Fluidization Velocity, Narrow Cuts Solids

Particle Diameter μm	Minimum Fluidizing Velocity						
	Calculated Equ.(6) (m/s.)	Calculated Equ.(7) (m/s.)	Calculated Equ.(11) (m/s.)	Experimental (m/s.)	% Error Equ.(6)	% Error Equ.(7)	% Error Equ.(11)
63	0.013	0.014	0.015	0.018	27.77	22.22	16.66
112	0.022	0.024	0.025	0.027	18.5	11.11	7.4
145	0.029	0.031	0.030	0.034	14.7	8.82	11.76

Table (5) gives the values of constant and powers for Wide Range Solids

C ₁	C ₂	C ₃
0.81	0.94	0.35

Where:- Proportion of variance accounted for: 0.846
 Correlation coefficient (R) = 0.92
 Average Absolute Relative Error (Error%) = 12.26
 Then the experimental data gives the following equation:-
 $Nu. = 0.81 Re^{0.94} Pr^{0.35}$
 For Wide Range Solids

Table (6) gives the values of constant and powers for Narrow Range Solids

C ₁	C ₂	C ₃
0.45	0.65	0.33

Where:- Proportion of variance accounted for: 0.7396
 Correlation coefficient (R) = 0.86
 Average Absolute Relative Error (Error%) = 24.2
 Then the experimental data gives the following equation:-
 $Nu. = 0.45 Re^{0.65} Pr^{0.33}$
 For Narrow Range Solids

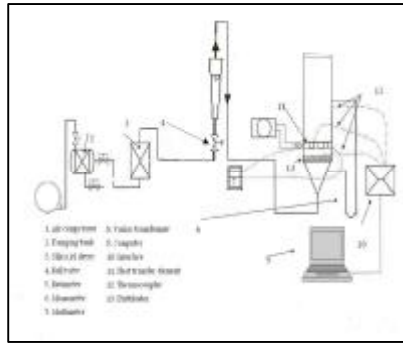


Figure (1) Schematic Diagram of the Experimental Setup

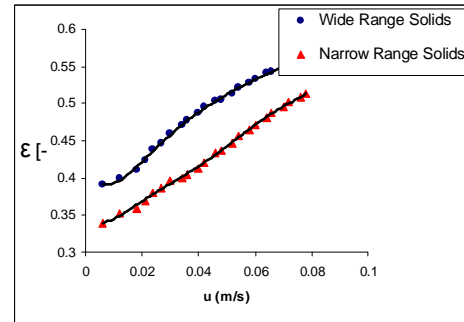


Figure (4) Variation in Voidage Fraction with Gas Fluidizing Velocity, for Sand Particle of 63 μ m



Figure (2) General View of Experimental Set up

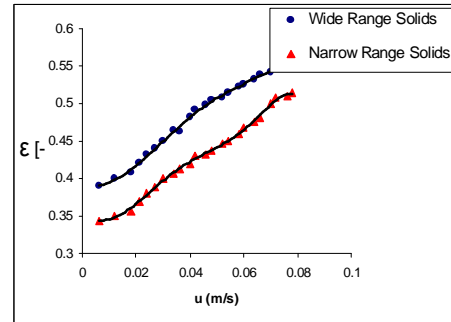


Figure (5) Variation in Voidage Fraction with Gas Fluidizing Velocity, for Sand Particle of 112 μ m

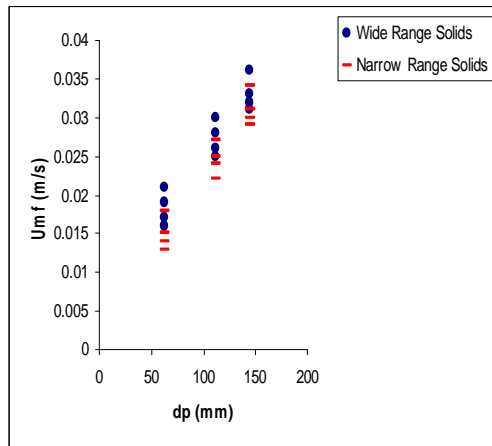


Figure (3) Variation in Minimum Fluidizing Velocity Experimental with Average Particle Diameter, for Different Measuring Techniques

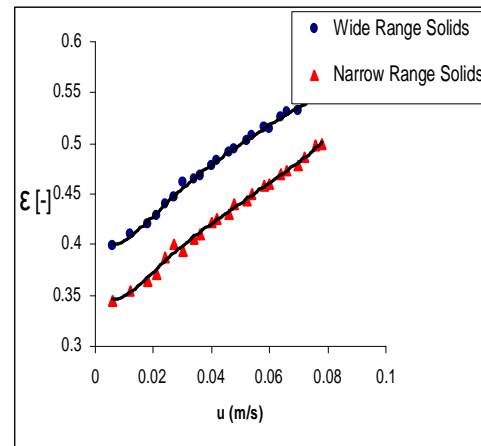


Figure (6) Variation in Voidage Fraction with Gas Fluidizing Velocity, for Sand Particle of 145 μ m

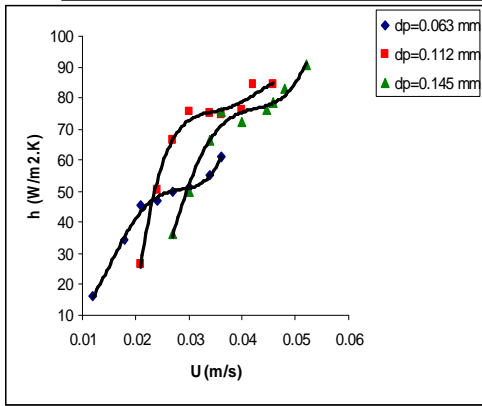


Figure (7) Heat Transfer Coefficient as a Function of Gas Fluidizing Velocity, Wide Range Solids for Different Sand Particle

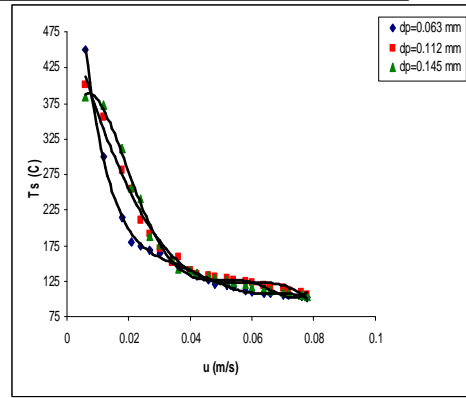


Figure (10) Variation in Surface Temperature with the Air Superficial Velocity for Different Particle Diameters, Wide Range Solids at Constant Heat Flux.

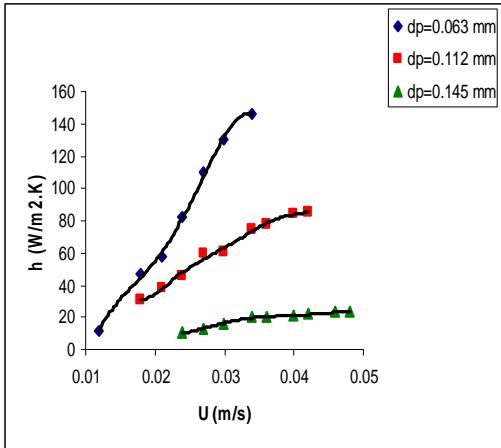


Figure (8) Heat Transfer Coefficient as a Function of Gas Fluidizing Velocity, Narrow Range Solids for Different Sand Particle

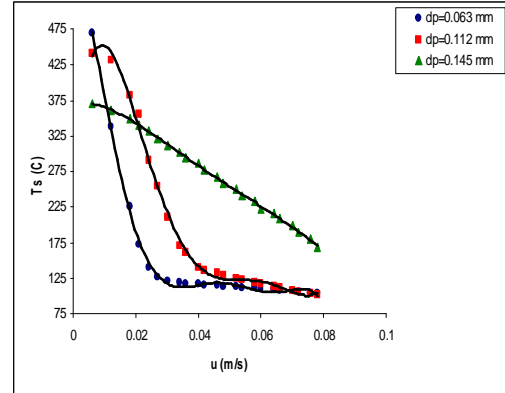


Figure (11) Variation in Surface Temperature with the Air Superficial Velocity for Different Particle Diameters, Narrow Range Solids at Constant Heat Flux.

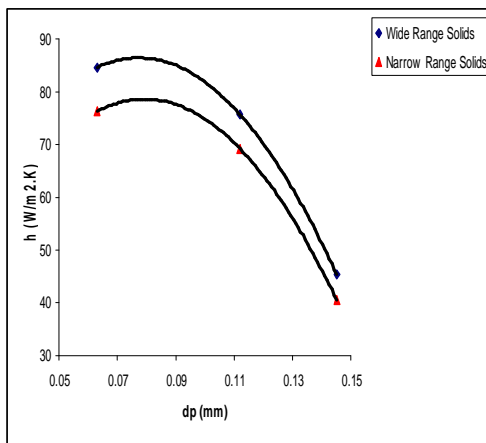


Figure (9) Variation of Surface-Bed Heat Transfer Coefficient with Average Particle Diameter, at Constant Heat Flux.

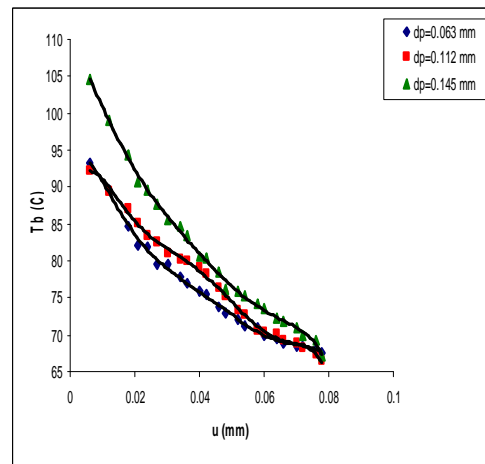


Figure (12) Variation in Bed Temperature with the Air Superficial Velocity for Different Particle Diameters, Wide Range Solids at Constant Heat Flux.

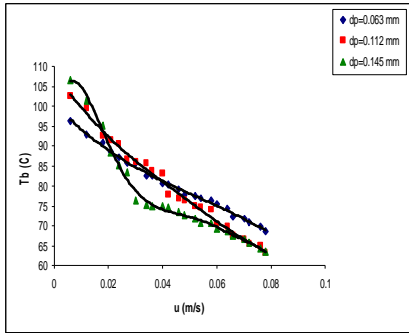


Figure (13) Variation in Bed Temperature with the Air Superficial Velocity for Different Particle Diameters, Narrow Range Solids at Constant Heat Flux.

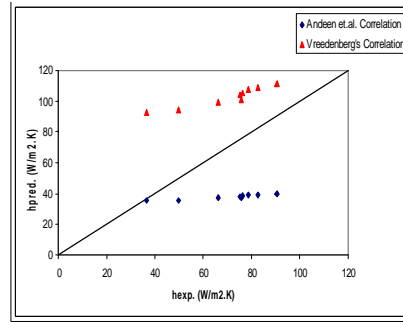


Figure (16) Comparison Between the Predicted Values of the Heat Transfer Coefficient and the Experimental h_w for Wide Range Solids ($dp=0.145$ mm)

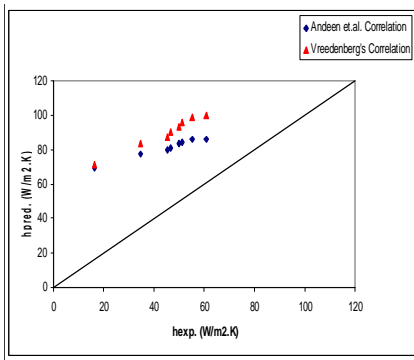


Figure (14) Comparison Between the Predicted Values of the Heat Transfer Coefficient and the Experimental h_w for Wide Range Solids ($dp=0.063$ mm)

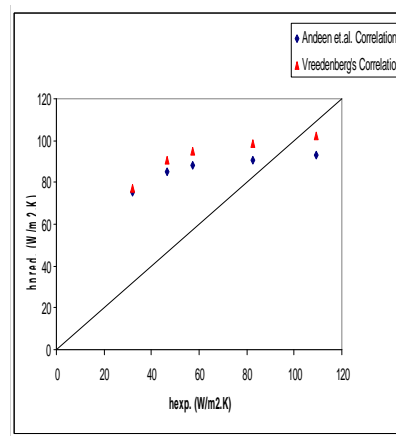


Figure (17) Comparison Between the Predicted Values of the Heat Transfer Coefficient and the Experimental h_w for Narrow Range Solids ($dp=0.063$ mm)

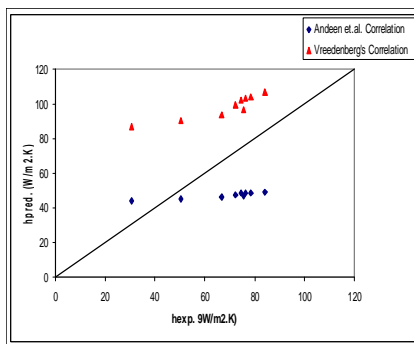


Figure (15) Comparison Between the Predicted Values of the Heat Transfer Coefficient and the Experimental h_w for Wide Range Solids ($dp=0.112$ mm)

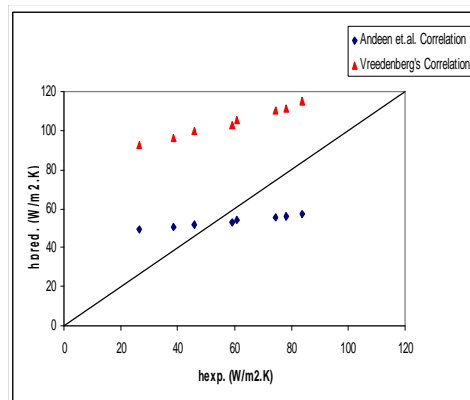


Figure (18) Comparison Between the Predicted Values of the Heat Transfer Coefficient and the Experimental h_w for Narrow Range Solids ($dp=0.112$ mm)

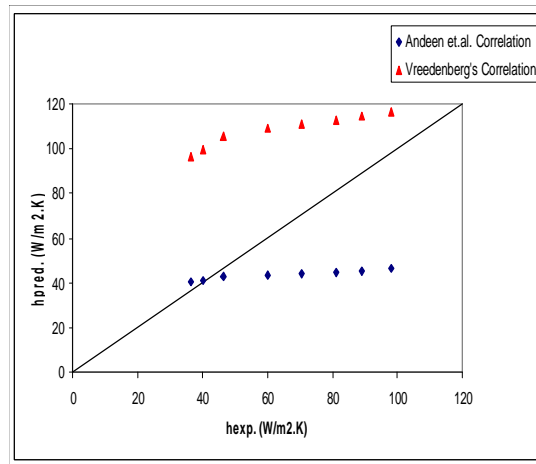


Figure (19) Comparison Between the Predicted Values of the Heat Transfer Coefficient and the Experimental h_c for Narrow Range Solids ($d_p=0.145$ mm)